

Volcanic eruption prediction: Magma chamber physics from gravity and deformation measurements

Hazel Rymer and Glyn Williams-Jones

Volcano Dynamics Group, Department of Earth Sciences, The Open University, Walton Hall, Milton Keynes, UK

Abstract. One of the greatest remaining problems in modern volcanology is the process by which volcanic eruptions are triggered. It is generally accepted that eruptions are preceded by magma intrusion [Sigurdsson and Sparks, 1978]. The degree of interaction between previously ponded magma in a chamber and newly intruded magma determines the nature and rate of eruption and also the chemistry of erupted lavas and shallow dykes. Here, we investigate the physics of this interaction. Volcano monitoring at its most effective is a synergy between basic science and risk assessment, while hazard mitigation depends on reliable interpretation of eruption precursors. The simple and much used Mogi model relates ground deformation (Δh) to changes in magma chamber volume. Gravity changes (Δg) combined with ground deformation provide information on magma chamber mass changes. Our new models predict how the $\Delta g/\Delta h$ gradient will evolve as a volcano develops from a state of dormancy through unrest into a state of explosive activity. Thus by simultaneous measurement of deformation and gravity at a few key stations, magma chamber processes can be identified prior to the onset of conventional eruption precursors.

Introduction

Conventional (high-precision) micro-gravity monitoring at active volcanoes is used to identify shallow processes within the feeder conduit using repeated Δg and Δh measurements at a network of stations in and around the active crater or caldera [Rymer, 1994; Rymer *et al.*, 1998a,b]. There are obvious risks associated with this practice and recent high profile cases of volcanologists being killed emphasise this point [Baxter and Gresham, 1997; Fujii and Nakada, 1999]. Monitoring volcanoes from a safe distance can entail reduced signal strength in the data. Other eruption pre-cursors such as tremors, gas flux/chemistry and temperature fluctuations reflect relatively shallow processes which are a source of noise in $\Delta g/\Delta h$ data in the active vent region. Processes within the magma chamber, which occur months or years before conventional pre-cursors, are interpreted here from $\Delta g/\Delta h$ data which may be obtained at some distance from the active vent, where the signal to noise ratio is enhanced. Hazard mitigation is thus greatly facilitated by the additional time afforded.

Observations

Ground deformation measurements have long been used to monitor active volcanoes [Murray *et al.*, 1995]. The volume

Copyright 2000 by the American Geophysical Union

Paper number 1999GL011293
0094-8276/00/1999GL011293\$05 00

of surface deformation (the change in edifice volume ΔV_e ; Figure 1) can be estimated from ground deformation measurements simply by integrating the observed height changes over the area of deformation. The Mogi [Mogi, 1958] model relates ΔV_e to the change in sub-surface magma chamber volume (ΔV_{ch}) assuming the country rocks to behave elastically and the magma chamber to behave as though it is a spherical pressure source whose depth is large compared with its radius. Without any other information, ground deformation provides no indication of the processes taking place inside the magma chamber. Variations in the acceleration due to gravity can also be monitored on active volcanoes and by integrating over the area of variations, the change in sub-surface magma mass (ΔM_m) can be quantified [Berrino *et al.*, 1992]. Simultaneous gravity and deformation measurements provide an estimate of ΔM_m and ΔV_{ch} so changes in the average density of the magma chamber may be deduced, providing insights into the process of vesiculation (density decrease) or crystallisation (density increase).

Deviations from the free air gradient (FAG) are due to sub-surface mass changes (Figure 2). When the density of the magma chamber is taken into account, the Bouguer corrected free air gradient (BCFAG) can be calculated. The value of the BCFAG depends on the model used - spherical source or slab [Berrino *et al.*, 1992; Rymer *et al.*, 1995]. Data plotting above the BCFAG on a $\Delta g/\Delta h$ graph (Figure 2) reflect density increases whereas data plotting below the BCFAG reflect density decreases. There is an interesting area between the FAG and the BCFAG where during inflation there are mass increases and density decreases and this is crucial to understanding the physics of magma chamber processes and the detection of eruption pre precursors.

Discussion

Micro-gravity and ground deformation surveys are frequently carried out in the region of maximum uplift, central to the volcanic region (zone A, Figure 1), in order to investigate relatively shallow sub surface processes. However sensitive instrumentation can detect the small off axis variations away from the active region (zone B, Figure 1). The advantage of making observations off axis is that the signal to noise ratio in the data is considerably increased as shallow volcanic effects within the edifice (vesiculation cycles within the feeder conduit, fracturing etc.; Rymer *et al.* [1998b]) are reduced. Another potential source of uncertainty is the variation in groundwater levels. The effects of water table fluctuations can be minimised by measuring gravity at stations located on crystalline bedrock [Jachens and Roberts, 1985] while seasonal variations in groundwater can be reduced by making measurements at approximately the same time every year [Rymer *et al.* 1995; Arnet *et al.*, 1997]. It is therefore possible to detect subtle changes within a Mogi-type magma

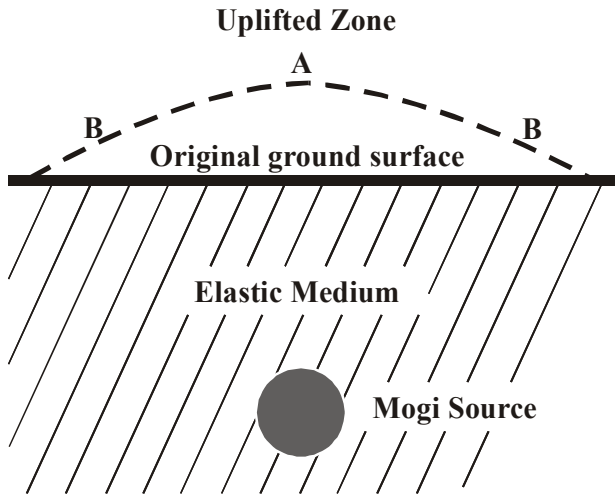


Figure 1. To a first approximation, a magma reservoir can be modelled as a spherical body. If the depth is large compared with its radius, the gravitational effect is that of a point source. The essence of the Mogi model is that dilation of a point source in an elastic half space causes deformation at the surface, which will depend on the amount of dilation and the elastic properties of the medium. By inserting measured or estimated values for the elastic properties of the surrounding rock, the amount of ground deformation measured at the surface by techniques such as GPS, SAR interferometry, altimetry or levelling, can therefore be used to estimate the change in sub-surface magma reservoir volume (ΔV_{ch}). The largest ground deformation changes are observed in zone A, but measurable effects are also seen in distal zones such as B. Gravity measurements may also be made at these points and when combined with ground deformation measurements, this is an extremely powerful method for investigating sub-surface density changes. Quantifying the magnitude and rate of these changes provides a means to detect eruption pre-cursors within the magma chamber, before the magma begins its journey through conduits to the surface, thus affording more time for hazard mitigation and evacuation.

chamber of 10^{11} kg to 10^{12} kg at 2-5 km depth at up to 3.5 km and 10 km horizontal distance, respectively. Although, the Mogi model represents an oversimplified magma chamber, many published geophysical data are consistent with this type of source [Berrino *et al.*, 1992; Arnet *et al.*, 1997; Avallone *et al.*, 1999]. Here we present two end member models that illustrate how, by observing density changes within the magma chamber, the hazard potential of a volcanic system can be determined.

Intruding magma with a relatively low Reynolds number (low velocity, high viscosity), as illustrated in model 1 (Figure 3), will interact very little with the chamber magma. There will be an overall mass increase in the system, which would be measurable at the surface as a gravity increase. The intrusion would produce some ground deformation and the $\Delta g/\Delta h$ gradient would fall into region 1 or along the BCFAG (Figure 2) indicating an overall increase in density (region 1) or no density change (BCFAG) within the magma chamber. Constant or increasing density within a magma chamber is indicative of a low potential hazard system, as magma is not

able to rise. In a closed system, the chamber will eventually stagnate, but if magma pressure exceeds the local lithostatic pressure, dykes may form which can in some cases eventually feed lava eruptions.

Model 2 assumes an intruding magma with a high Reynolds number which will interact with the chamber magma, heating it and inducing vesiculation (Figure 3). This results in a net subsurface mass increase and density decrease observable at the surface as a $\Delta g/\Delta h$ relationship falling into region 2, between the FAG and BCFAG (Figure 2). In this case, the interaction [Sparks *et al.*, 1980] between the intruding magma and the older magma is critically, more pervasive than in model 1. Magma mixing and mingling will cause significant bubble formation. The build up of gas pressure within a magma chamber is an essential precursor to eruptive activity [Woods and Koyaguchi, 1994] and has considerable hazard implications.

We infer from these models that as a volcano develops

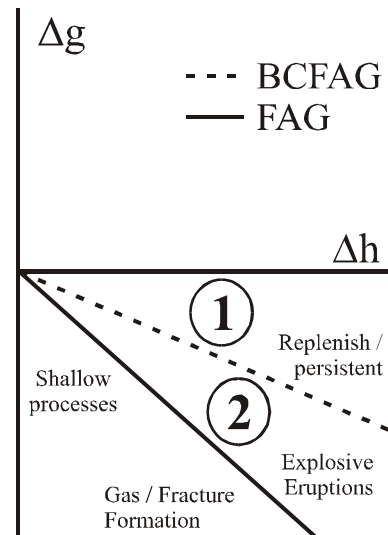


Figure 2. During periods of inflation, increasing elevation (Δh) is accompanied by decreasing gravity (negative Δg), described by the BCFAG. For the Mogi model and for an infinite Bouguer slab, the relationship is linear. For other models (e.g., dyke, sill etc.), the relationship is not linear, but $\Delta g/\Delta h$ data will fall between the BCFAG lines for these two end member models. The actual gradient of the BCFAG will depend on the density assumed for the surrounding rock. It ranges from $-224 \mu\text{Gal m}^{-1}$ to $-252 \mu\text{Gal m}^{-1}$ for a density of 2000 kg m^{-3} and $-113 \mu\text{Gal m}^{-1}$ to $-233 \mu\text{Gal m}^{-1}$ for a density of 2700 kg m^{-3} for the slab and sphere models respectively. The free air gradient (FAG) is typically $-308.6 \mu\text{Gal m}^{-1}$, but may vary by about 10% depending on the local terrain and Bouguer anomaly [Rymer, 1994]. Thus the BCFAG is model dependent and the FAG should always be measured. Region 1 represents anomalously large gravity increases accompanying inflation and could be interpreted in terms of magma intrusion increasing the average density of the magma chamber. Data falling into region 2 reflect density decrease and mass increase during inflation (and volume increase) which we interpret in terms of the build up of gas within the magma chamber – the most likely trigger process for an eruption. Data falling close to the Δg line reflect shallow processes such as magma and gas fluctuations within the feeder conduit or may not even be of immediate volcanological interest (e.g., water table level excursions).

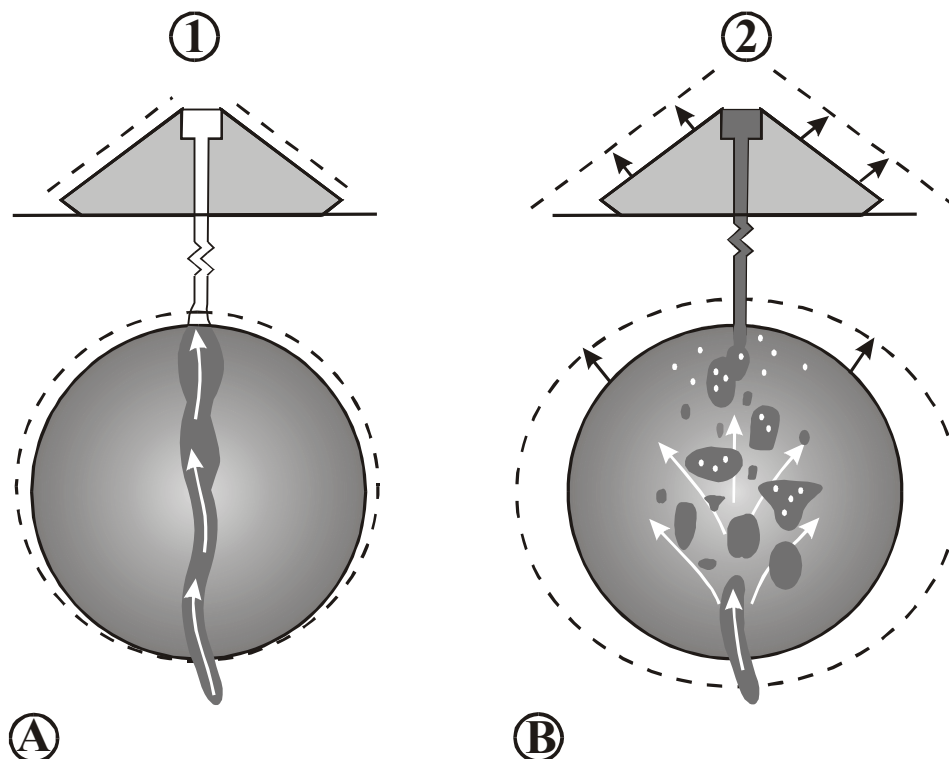


Figure 3. A. Model 1 depicts a low Reynolds number magma (relatively low velocity and high viscosity) entering a magma chamber and not interacting significantly with the surrounding magma. B. Model 2 has the same magma mass influx as model 1, but the Reynolds number is higher. In this case, the magma interacts with the surrounding magma, heating it, and causing vesiculation and expansion of the chamber. In model 1 the $\Delta g/\Delta h$ gradient will fall into region 1 of Figure 2; in model 2, the gradient will fall into region 2 of Figure 2.

from a state of dormancy through unrest into eruptive activity, that the $\Delta g/\Delta h$ gradient will evolve away from the BCFAG towards the FAG. The application of this to hazard warning is as follows. As the gradient varies from region 1 towards the BCFAG, the density of the magma chamber decreases (Figure 2). This would be a result of reduced crystallisation and increased buoyant melt and vesicle content. Once the BCFAG is crossed, the density of the magma chamber has decreased below the previous average value of the chamber and the system becomes unstable. It is at this stage that the magma will be able to rise. If there is limited heating, then magma convection within the chamber (recently linked with pulses of activity at the surface [Kazahaya *et al.*, 1994]) will follow, but with excess heating, as gas pressure increases, the likelihood of an eruption increases [Woods and Koyaguchi, 1994].

Conclusions

Target areas are calderas in a state of unrest and large composite volcanoes. An open magmatic system is one that displays persistent surface manifestations ranging from a stable lava lake to explosive eruptions and vigorous fumarolic activity. At these systems measurements made in region A (Figure 1) will be dominated by shallow processes. In order to investigate processes within a Mogi-type source and to increase the signal to noise ratio from this source, measurements must be made in region B. A closed system on the other hand, has little or no surface activity and therefore $\Delta g/\Delta h$ gradient measurements may be made safely in both regions A and B. A prime example of a closed system is the

Campi Flegrei caldera (Naples, Italy) which was characterised by a bradyseismic crisis in the early 1980s. The average $\Delta g/\Delta h$ gradient ($-213 \pm 6 \mu\text{Gal m}^{-1}$) during inflation, measured at stations in regions A and B, fell into region 1 (Figure 2). As our model predicts, there was no eruption. Indeed, as data in Berrino [1994] show, the gradient actually evolved (February 1981 to March 1983) from the BCFAG towards the horizontal axis, well within region 1 (Figure 2). This episode was interpreted in terms of intrusion into a magma chamber [Berrino *et al.*, 1984] or mobilisation of the hydrothermal system [Bonafede, 1991]. Our model predicts that if the $\Delta g/\Delta h$ gradient steepens beyond $-220 \mu\text{Gal m}^{-1}$ during inflation an eruption will follow (Table 1). Given the considerable history of caldera unrest at Campi Flegrei and the increasing population of the region, there is a vital need to distinguish between magma chamber processes such as those presented here in models 1 and 2 (Figure 3).

Data from Campi Flegrei, Rabaul and Long Valley all fall into region 1 of our model (Table 1). This is consistent with the fact that no eruption occurred at these sites. The Krafla data on the other hand fall within region 2 and are consistent with the eruption that followed. The actual value of the BCFAG will depend on the FAG, the Bouguer anomaly and the density of the intrusion [Rymer, 1994]. However even if the theoretical values for the FAG ($-308 \mu\text{Gal m}^{-1}$) and the BCFAG ($-233 \mu\text{Gal m}^{-1}$ for a density of 2700 kg m^{-3}) are used, the data from all the published examples still fall into the same regions.

Simultaneous measurements of deformation and gravity at a few key stations may therefore be used to identify magma

Table 1. Summary of rigorously documented gravity-height changes observed during inflation and associated with caldera unrest.

Volcano	Inflationary Period	$\Delta g/\Delta h$ (μGal)	FAG ($\mu\text{Gal m}^{-1}$)	BCFAG ($\mu\text{Gal m}^{-1}$)
Campei Flegrei <i>Italy</i>	Feb. 1981- Mar. 1983	-213 ± 6^a	-290 ± 5^a	-220^a
Rabaul <i>PNG</i>	1973-1985	-216 ± 4^b	-300^a	-238^a
Krafla <i>Iceland</i>	Jan.-June 1978	-250 ± 20^c	-308^*	-200^d
Long Valley <i>USA</i>	1982-1998	-215 ± 11^e	-308^*	-233^*

^a Berrino et al. (1992); ^b McKee et al. (1989); ^c Johnson et al. (1980); ^d Rymer et al. (1998a); ^e Battaglia et al. (1999)

* Theoretical

chamber processes prior to the onset of conventional eruption precursors. The method is expected to find greatest application in regions where a Mogi type chamber is located at 2-5 km depth, where the magma system is essentially closed and where early hazard warning is essential.

Acknowledgements. This research was supported by the Royal Society, The Open University Research Development Fund and NERC. We are grateful to C. A. Locke, J. Cassidy and J. B. Murray for helpful discussions. This work was greatly improved by the comments of G. Berrino and A.T. Linde.

References

- Arnet, F., H.-G. Kahle, E. Klingelé, R. B. Smith, C. M. Meertens and D. Dzurisin, Temporal gravity and height changes of the Yellowstone caldera, 1977 – 1994, *Geophys. Res. Lett.*, **24**, 2741-2744, 1997.
- Avallone, A., A. Zollo, P. Briole, C. Delacourt and F. Beauducel, Subsidence of Campi Flegrei (Italy) detected by SAR interferometry, *Geophys. Res. Lett.*, **26**, 2303-2306, 1999.
- Battaglia, M., C. Roberts and P. Segall, Magma intrusion beneath Long Valley caldera confirmed by temporal changes in gravity, *Science*, **285**: 2119-2122, 1999.
- Baxter, P. J. and A. Gresham, Deaths and injuries in the eruption of Galeras Volcano, Colombia, 14 January 1993, *J. Volcanol. Geotherm. Res.*, **77**, 325-338, 1997.
- Berrino, G., G. Corrado, G. Luongo and B. Toro, Ground deformation and gravity changes accompanying the 1982 Pozzuoli uplift, *Bull. Volcanol.*, **47**, 187-200, 1984.
- Berrino, G., H. Rymer, G. C. Brown and G. Corrado, Gravity-height correlations for unrest at calderas, *J. Volcanol. Geotherm. Res.*, **53**, 11-26, 1992.
- Berrino, G., Gravity changes induced by height-mass variations at the Campi Flegrei caldera, *J. Volcanol. Geotherm. Res.*, **61**, 293-309, 1994.
- Bonafede, M., Hot fluid migration; an efficient source of ground deformation; application to the 1982-1985 crisis at Campi Flegrei-Italy, *J. Volcanol. Geotherm. Res.*, **48**, 187-198, 1991.
- Fujii, T. and S. Nakada, The 15 September 1991 pyroclastic flows at Unzen Volcano (Japan); a flow model for associated ash-cloud surges, *J. Volcanol. Geotherm. Res.*, **89**, 159-172, 1999.
- Jachens, R. C. and C. W. Roberts, Temporal and areal gravity investigations at Long Valley Caldera, California, *J. Geophys. Res.*, **90**, 11210-11218, 1985.
- Johnson, G. V., A. Björnsson and S. Sigurdsson, Gravity and elevation changes caused by magma movement beneath the Krafla caldera, Northeast Iceland, *J. Geophys. Res.*, **47**, 132-140, 1980.
- Kazahaya, K., H. Shinohara and G. Saito, Excessive degassing of Izu-Oshima volcano: magma convection in a conduit, *Bull. Volcanol.*, **56**, 207-216, 1994.
- McKee, C., J. Mori and Talai, B. Microgravity changes and ground deformation at Rabaul Caldera, 1973-1985, In: IAVCEI Proceedings in Volcanology 1, J.H. Latter (Ed.), Volcanic Hazards, Springer-Verlag, Berlin, 399-428, 1989.
- Mogi, K. Relations between the eruptions of various volcanoes and the deformations of the ground surfaces around them, *Bull. Earthquake. Res. Inst.*, **36**, 99-134, 1958.
- Murray, J. B., A. D. Pullen and S. Saunders, Ground deformation surveying of active volcanoes, In *Monitoring Active Volcanoes*, McGuire, B.; C. R. J. Kilburn, and J. B. Murray (Eds.), UCL Press, London, 113-150, 1995.
- Rymer, H. Microgravity changes as a precursor to volcanic activity, *J. Volcanol. Geotherm. Res.*, **61**, 311-328, 1994.
- Rymer, H., J. Cassidy, C. A. Locke and F. Sigmundsson, Post-eruptive gravity changes from 1990 to 1996 at Krafla Volcano, Iceland, *J. Volcanol. Geotherm. Res.*, **87**, 141-149, 1998a.
- Rymer, H., B. van Wyk de Vries, J. Stix and G. Williams-Jones, Pit crater structure and processes governing persistent activity at Masaya Volcano, Nicaragua, *Bull. Volcanol.*, **59**, 345-355, 1998b.
- Rymer, H., J. Cassidy, C. A. Locke and J. B. Murray, Magma movements in Etna volcano associated with the major 1991-1993 lava eruption: evidence from gravity and deformation, *Bull. Volcanol.*, **57**, 451-461, 1995.
- Sigurdsson, H. and R. S. J. Sparks, Rifting episode in North Iceland in 1874-1875 and the eruptions of Askja and Sveinagja, *Bull. Volcanol.*, **41**, 149-167, 1978.
- Sparks, R. S. J., P. Meyer and H. Sigurdsson, Density variation amongst Mid-Ocean Ridge basalts: Implications for magma mixing and the scarcity of primitive lavas, *Earth Planet. Sci. Lett.*, **46**: 419-430, 1980.
- Woods, A. W. and T. Koyaguchi, Transitions between explosive and effusive eruptions of silicic magmas, *Nature*, **370**, 641-644, 1994.

H. Rymer and G. Williams-Jones, Volcano Dynamics Group, Department of Earth Sciences, The Open University, Walton Hall, Milton Keynes, MK7 6AA, UK (e-mail: h.rymer@open.ac.uk)

(Received: December 13, 1999; revised: May 25, 2000; accepted: June 26, 2000)